Supplemental Information: Preparation of an Exciton Condensate of Photons on a 53-Qubit Quantum Computer

LeeAnn M. Sager, Scott E. Smart, and David A. Mazziotti*
Department of Chemistry and The James Franck Institute, The University of Chicago, Chicago, IL 60637

I. THE LIPKIN HAMILTONIAN

One of the simplest and most well-known models for exciton condensation is the Lipkin model in the large-coupling regime [1–5]. The Lipkin quasispin model consists of N fermions distributed over two, N-fold degenerate levels with energies $-\epsilon$ and ϵ where the particles have a pairwise "monopole-monopole" interaction with strength V, which scatters the pairs between the two levels. The Hamiltonian for this model is given by

$$\hat{H} = \epsilon \hat{J}_z + \frac{V}{2}\left(\hat{J}^2_{+,-} + \hat{J}^2_{-,+}\right) \tag{SI-1}$$

where

$$\hat{J}_z = \frac{1}{2}\sum_m m \sum_{p=1}^{N} \hat{a}^\dagger_{m,p}\hat{a}_{m,p}, \tag{SI-2}$$

$$\hat{J}_{+,-} = \sum_{p=1}^{N} \hat{a}^\dagger_{+1,p}\hat{a}_{-1,p}, \tag{SI-3}$$

$$\hat{J}_{-,+} = \sum_{p=1}^{N} \hat{a}^\dagger_{-1,p}\hat{a}_{+1,p}, \tag{SI-4}$$

$\hat{a}^\dagger$ and $\hat{a}$ are fermionic creation and annihilation operators, $m(\pm 1)$ denotes the two levels, and ϵ and V are parameters. Note that from this representation, it is apparent that each orbital in the bottom layer has a corresponding orbital in the top layer to which they are particle-hole paired (i.e., only vertical transitions are allowed). Additionally, the parameter V controls the relative importance of of two particle interactions such that a large V indicates that the two-body part of the Hamiltonian is dominant—the large-coupling limit for which exciton condensation is known to occur.

*Electronic address: damazz@uchicago.edu

II. CALIBRATION DATA FOR IBM QUANTUM DEVICES EMPLOYED

TABLE I: Calibration data for "Yorktown"

Device:	ibmqx2 ("Yorktown")						
Calibration Date:	9/17/19						
Version:	2.0.0						
Gate time (ns):	71.1						
Qubit:		0	1	2	3	4	
	T2 (μs)	44.9	40.4	76.5	25.9	44.5	
	f (GHz)	5.29	5.24	5.03	5.30	5.08	
	T1 (μs)	58.1	48.3	62.0	60.2	65.5	
	Gate Error (10^{-3})	0.87	1.08	0.75	0.95	1.23	
	Readout Error (10^{-3})	10.5	12.0	12.5	15.0	23.0	
Multi-Qubit:		0,1	0,2	1,2	3,2	3,4	4,2
	Error (10^{-3})	14.9	15.0	25.2	14.1	25.3	16.8

TABLE II: Calibration data for “Melbourne”

Device:	ibmq_16_melbourne (“Melboure”)																						
Calibration Date:	1/10/20																						
Version:	2.0.0																						
Gate time (ns):	53.3																						
Qubit:		0	1	2	3	4	5	6	7	8	9	10	11	12	13	14							
	T2 (μs)	16.8	78.5	137.1	50.5	34.5	52.5	67.7	79.2	129.2	82.1	47.2	100.2	9.3	52.3	50.3							
	f (GHz)	5.10	5.24	5.03	4.90	5.03	5.07	4.92	4.97	4.74	4.96	4.95	5.01	4.76	4.97	5.00							
	T1 (μs)	73.6	63.4	78.5	83.0	64.7	21.9	58.5	60.8	89.2	44.8	74.9	39.9	5.7	30.7	46.0							
	Gate Error (10^{-3})	0.44	1.00	0.39	0.34	0.83	2.12	1.03	1.49	0.97	1.84	2.07	0.58	4.97	2.96	0.65							
	Readout Error (10^{-3})	28.5	23.5	18	136	23.5	70	107.5	124	142	13.5	68	32.5	157.5	305.5	40							
Multi-Qubit:		0,1	0,14	1,2	1,13	2,3	2,12	3,4	3,11	4,5	4,10	5,6	5,9	6,8	7,8	8,9	9,10	10,11	11,12	12,13	13,14		
	Error (10^{-3})	23.6	26.2	11.7	1000.0	15.9	46.2	18.0	26.7	24.7	38.8	34.4	32.3	25.3	30.4	33.6	42.7	26.3	53.9	125.8	66.3		

TABLE III: Calibration data for "Rochester"

Device:	ibmq_rochester ("Rochester")																				
Calibration Date:	2/26/20																				
Version:	1.2.0																				
Gate time (ns):	53.3																				
Qubit:		0	1	2	3	4	5	6	7	8	9	10	11	12	13	14	15	16	17	18	19
	T2 (μs)	81.1	69.1	65.3	45.5	68.7	68.8	52.1	53.1	61.0	81.3	101.3	24.9	54.9	97.6	38.0	24.9	75.0	10.3	53.3	45.8
	f (GHz)	4.92	5.08	5.00	5.05	4.94	5.05	5.05	4.93	5.03	4.97	5.06	4.93	5.05	4.95	5.07	4.87	5.08	4.99	5.06	5.02
	T1 (μs)	46.1	51.5	49.2	20.4	42.2	53.5	54.5	43.5	44.8	59.1	65.3	21.1	45.9	63.3	44.4	55.2	59.5	42.8	35.7	48.6
	Gate Error (10^{-3})	4.94	0.65	2.27	5.68	7.44	1.20	1.57	0.76	1.82	1.01	0.85	1.35	2.69	0.89	1.01	0.82	0.64	1.15	0.75	0.75
	Readout Error (10^{-3})	32.5	68.1	227.5	120.0	66.3	235.0	58.7	91.3	105.0	138.1	59.4	100.0	152.5	349.4	135.0	91.9	56.9	50.6	35.0	250.0
		20	21	22	23	24	25	26	27	28	29	30	31	32	33	34	35	36	37	38	39
	T2 (μs)	58.9	31.6	13.5	49.7	32.5	82.0	54.9	75.7	68.8	22.0	64.7	85.0	68.3	56.9	21.1	45.9	54.7	119.6	88.3	52.4
	f (GHz)	5.06	5.02	4.89	5.14	4.90	4.96	4.88	4.97	5.02	4.99	5.02	5.00	5.11	4.96	5.15	5.21	4.97	5.04	5.03	5.17
	T1 (μs)	36.9	30.3	59.7	62.7	60.7	67.6	60.6	55.7	50.2	54.4	60.5	60.0	66.4	50.8	62.2	46.1	51.0	66.3	85.1	39.1
	Gate Error (10^{-3})	0.68	1.74	1.50	1.80	1.19	1.08	1.09	1.14	0.98	1.79	3.15	0.72	2.39	0.80	2.20	3.78	2.36	0.60	0.66	2.46
	Readout Error (10^{-3})	19.4	82.5	89.4	166.9	14.4	32.5	73.1	158.1	123.1	26.9	306.9	143.1	285.6	37.5	228.1	171.2	31.3	135.6	211.2	136.2
		40	41	42	43	44	45	46	47	48	49	50	51	52							
	T2 (μs)	87.7	72.4	77.0	31.3	41.0	39.5	78.4	55.6	98.1	65.5	35.6	23.1	91.0							
	f (GHz)	5.06	5.05	4.99	5.07	4.97	5.09	5.03	5.07	4.97	5.07	4.96	5.13	5.04							
	T1 (μs)	57.2	61.6	60.9	45.3	67.7	60.4	51.4	52.8	57.0	56.2	49.0	42.7	67.0							
	Gate Error (10^{-3})	1.18	1.94	0.83	1.91	19.09	2.21	1.62	1.59	1.12	0.98	0.90	14.39	5.45							
	Readout Error (10^{-3})	102.5	70.6	43.1	106.2	115.0	109.4	48.7	210.6	20.6	71.9	85.6	190.6	136.9							
Multi-Qubit:		0,1	0,5	1,2	2,3	3,4	4,6	5,9	6,13	7,8	7,16	8,9	9,10	10,11	11,12	11,17	12,13	13,14	14,15	15,18	16,19
	Error (10^{-3})	46.5	63.0	21.7	56.4	85.6	1000.0	31.7	47.5	1000.0	29.5	33.8	23.1	23.0	59.3	25.8	45.4	54.5	45.7	40.1	25.6
		17,23	18,27	19,20	20,21	21,22	21,28	22,23	23,24	24,25	25,26	25,29	26,27	29,26	30,31	30,39	31,32	32,33	33,34	34,35	34,40
	Error (10^{-3})	58.8	28.9	19.1	25.2	83.3	33.0	65.4	28.6	47.5	46.5	143.4	34.1	51.4	40.0	72.2	45.7	29.3	1000.0	92.8	28.1
		35,36	36,37	37,38	38,41	39,42	40,46	41,50	42,43	43,44	44,45	44,51	45,46	46,47	47,48	48,49	48,52	49,50			
	Error (10^{-3})	36.4	39.8	23.8	187.0	52.9	36.2	41.5	21.3	1000.0	1000.0	1000.0	56.5	26.4	23.0	33.3	64.8	26.9			

III. ORBITAL OCCUPATION NUMBER AND EIGENVALUE DATA

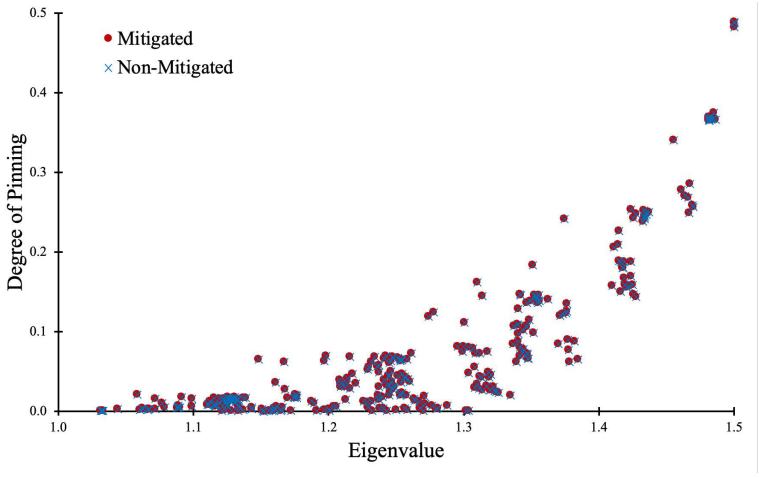

(a)Simulation

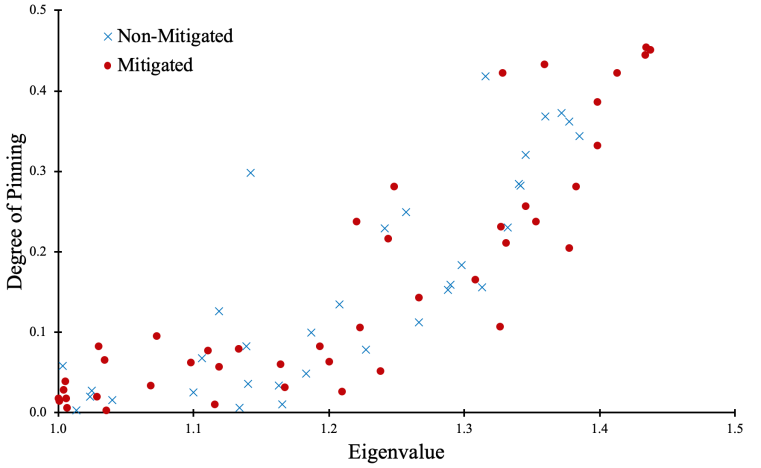

(b)Mitigated

FIG. 1: **Exciton Condensation Data.** The eigenvalues, independent orbital occupation numbers, and degree of pinning for the (a) simulated and (b) experimental data.

TABLE IV: Data from Three-Qubit, Simulated Calculations

Eigenvalue	**Degree of Pinning**	n_4	n_5	n_6
1.002	0.000	0.146	0.145	0.000
1.002	0.000	0.016	0.016	0.000
1.003	0.000	0.015	0.015	0.000
1.003	0.000	0.484	0.484	0.000
1.003	0.000	0.365	0.365	0.000
1.003	-0.001	0.000	0.000	0.000
1.004	0.000	0.151	0.151	0.000
1.005	0.000	0.253	0.253	0.000
1.005	0.000	0.073	0.073	0.000
1.005	0.000	0.493	0.493	0.000
1.006	0.000	0.485	0.485	0.000
1.006	0.000	0.065	0.065	0.000
1.006	0.000	0.245	0.245	0.000
1.006	0.000	0.066	0.066	0.000
1.007	0.000	0.254	0.253	0.000

1.007	0.000	0.484	0.484	0.000
1.007	0.000	0.481	0.481	0.000
1.007	0.000	0.492	0.492	0.000
1.007	0.000	0.489	0.489	0.000
1.007	0.000	0.490	0.490	0.000
1.008	0.000	0.373	0.372	0.000
1.009	0.000	0.141	0.141	0.000
1.011	0.000	0.497	0.497	0.000
1.011	0.000	0.017	0.017	0.000
1.012	0.000	0.377	0.377	0.000
1.032	0.001	0.372	0.372	0.001
1.032	0.001	0.032	0.018	0.015
1.033	0.000	0.029	0.015	0.014
1.033	0.001	0.033	0.018	0.016
1.044	0.003	0.082	0.069	0.016
1.058	0.021	0.036	0.034	0.023
1.061	0.002	0.077	0.063	0.016
1.062	0.003	0.382	0.381	0.004
1.062	0.003	0.258	0.258	0.004
1.066	0.001	0.078	0.063	0.016
1.067	0.003	0.078	0.064	0.017
1.067	0.002	0.081	0.067	0.016
1.072	0.015	0.085	0.083	0.017
1.072	0.003	0.081	0.069	0.015
1.077	0.010	0.155	0.154	0.011
1.079	0.005	0.163	0.151	0.017
1.088	0.004	0.159	0.146	0.018
1.089	0.005	0.156	0.144	0.017
1.089	0.007	0.413	0.413	0.008
1.089	0.004	0.157	0.146	0.015
1.090	0.005	0.161	0.147	0.018
1.092	0.018	0.078	0.061	0.035
1.099	0.015	0.082	0.063	0.035
1.099	0.006	0.153	0.140	0.019
1.111	0.008	0.254	0.244	0.018
1.111	0.009	0.263	0.255	0.017
1.111	0.008	0.255	0.247	0.017
1.112	0.013	0.437	0.435	0.014
1.115	0.008	0.127	0.069	0.066
1.115	0.016	0.284	0.282	0.019
1.116	0.008	0.257	0.249	0.016
1.116	0.007	0.254	0.244	0.017
1.116	0.006	0.120	0.081	0.045
1.117	0.008	0.155	0.129	0.034
1.119	0.011	0.123	0.067	0.067
1.120	0.015	0.492	0.491	0.016
1.121	0.001	0.196	0.158	0.039
1.121	0.007	0.127	0.068	0.066
1.122	0.015	0.487	0.482	0.019
1.122	0.016	0.490	0.490	0.016
1.123	0.016	0.486	0.486	0.016
1.123	0.001	0.286	0.263	0.024
1.124	0.012	0.380	0.375	0.016
1.125	0.007	0.125	0.082	0.049
1.125	0.008	0.254	0.245	0.017
1.125	0.014	0.373	0.369	0.017
1.125	0.016	0.490	0.488	0.018
1.126	0.015	0.380	0.376	0.019
1.126	0.018	0.493	0.492	0.020
1.127	0.015	0.486	0.484	0.017
1.127	0.013	0.367	0.363	0.018
1.128	0.014	0.388	0.383	0.018
1.128	0.015	0.491	0.490	0.016
1.128	0.000	0.278	0.254	0.024

1.129	0.016	0.494	0.493	0.017
1.129	0.015	0.493	0.492	0.016
1.129	0.015	0.373	0.371	0.017
1.130	0.016	0.464	0.462	0.018
1.130	0.016	0.486	0.484	0.018
1.130	0.018	0.495	0.494	0.018
1.131	0.012	0.163	0.137	0.037
1.132	0.015	0.495	0.495	0.015
1.132	0.014	0.491	0.490	0.015
1.133	0.007	0.392	0.380	0.018
1.133	0.015	0.490	0.490	0.016
1.133	0.000	0.187	0.156	0.032
1.134	0.005	0.386	0.375	0.015
1.137	0.002	0.407	0.383	0.026
1.137	0.016	0.485	0.484	0.018
1.139	0.017	0.491	0.490	0.017
1.143	0.005	0.255	0.225	0.036
1.143	0.003	0.407	0.390	0.020
1.148	0.065	0.094	0.081	0.079
1.151	0.003	0.252	0.222	0.033
1.152	0.000	0.427	0.403	0.025
1.152	0.000	0.195	0.113	0.082
1.156	0.000	0.379	0.347	0.032
1.156	0.001	0.193	0.114	0.080
1.159	0.001	0.435	0.407	0.029
1.160	0.000	0.470	0.440	0.030
1.160	0.001	0.474	0.441	0.033
1.160	0.004	0.491	0.459	0.036
1.160	0.004	0.495	0.464	0.035
1.161	0.036	0.192	0.190	0.038
1.162	0.006	0.487	0.460	0.033
1.164	0.000	0.318	0.278	0.040
1.165	0.002	0.384	0.351	0.034
1.166	0.005	0.490	0.460	0.035
1.167	0.062	0.130	0.130	0.062
1.168	0.028	0.314	0.313	0.029
1.170	0.017	0.193	0.142	0.068
1.172	0.001	0.317	0.282	0.036
1.175	0.018	0.195	0.146	0.067
1.175	0.017	0.191	0.141	0.066
1.175	0.021	0.198	0.150	0.069
1.177	0.019	0.190	0.143	0.066
1.177	0.017	0.192	0.145	0.063
1.188	0.012	0.255	0.190	0.078
1.189	0.010	0.253	0.195	0.068
1.191	0.001	0.291	0.209	0.083
1.197	0.002	0.246	0.161	0.087
1.197	0.063	0.161	0.145	0.078
1.198	0.069	0.155	0.140	0.084
1.200	0.003	0.254	0.160	0.098
1.201	0.000	0.282	0.202	0.080
1.204	0.006	0.375	0.324	0.057
1.206	0.006	0.369	0.321	0.055
1.208	0.039	0.190	0.123	0.106
1.209	0.030	0.283	0.251	0.062
1.209	0.035	0.192	0.124	0.103
1.212	0.031	0.280	0.248	0.063
1.213	0.015	0.328	0.259	0.083
1.214	0.036	0.289	0.260	0.065
1.214	0.041	0.282	0.253	0.070
1.216	0.069	0.253	0.252	0.071
1.216	0.029	0.286	0.252	0.062
1.218	0.046	0.376	0.375	0.047
1.221	0.035	0.282	0.253	0.064

1.226	0.013	0.328	0.268	0.073
1.229	0.011	0.390	0.317	0.085
1.229	0.005	0.382	0.308	0.080
1.229	0.052	0.254	0.226	0.080
1.230	0.056	0.259	0.233	0.081
1.231	0.062	0.442	0.441	0.063
1.232	0.012	0.431	0.377	0.066
1.232	0.001	0.326	0.195	0.132
1.234	0.068	0.488	0.486	0.070
1.236	0.056	0.494	0.489	0.061
1.236	0.020	0.284	0.178	0.126
1.237	0.016	0.477	0.418	0.076
1.237	0.014	0.443	0.383	0.075
1.237	0.031	0.434	0.392	0.073
1.237	0.057	0.389	0.375	0.071
1.238	0.049	0.378	0.362	0.066
1.238	0.004	0.366	0.270	0.100
1.240	0.017	0.277	0.171	0.124
1.241	0.004	0.377	0.287	0.094
1.241	0.039	0.409	0.374	0.074
1.241	0.066	0.491	0.490	0.066
1.243	0.070	0.487	0.486	0.070
1.243	0.032	0.386	0.332	0.087
1.243	0.001	0.315	0.191	0.125
1.245	0.044	0.250	0.150	0.144
1.245	0.061	0.491	0.490	0.061
1.245	0.045	0.384	0.366	0.064
1.245	0.020	0.489	0.426	0.083
1.245	0.033	0.372	0.322	0.083
1.246	0.024	0.495	0.434	0.086
1.246	0.063	0.494	0.493	0.064
1.246	0.050	0.380	0.367	0.062
1.247	0.037	0.327	0.252	0.112
1.247	0.067	0.492	0.491	0.068
1.248	0.027	0.491	0.441	0.077
1.248	0.068	0.493	0.492	0.070
1.248	0.032	0.414	0.379	0.067
1.249	0.031	0.486	0.436	0.081
1.250	0.002	0.439	0.328	0.113
1.251	0.067	0.494	0.491	0.070
1.251	0.045	0.387	0.368	0.065
1.253	0.065	0.486	0.484	0.067
1.253	0.020	0.463	0.407	0.076
1.253	0.063	0.495	0.492	0.067
1.253	0.022	0.443	0.394	0.070
1.254	0.066	0.492	0.491	0.066
1.254	0.036	0.490	0.438	0.088
1.254	0.047	0.380	0.362	0.065
1.255	0.064	0.495	0.492	0.067
1.255	0.023	0.494	0.438	0.080
1.256	0.041	0.487	0.442	0.086
1.256	0.044	0.258	0.156	0.146
1.257	0.003	0.389	0.262	0.130
1.257	0.020	0.491	0.428	0.083
1.258	0.065	0.495	0.495	0.065
1.258	0.001	0.431	0.314	0.118
1.259	0.040	0.242	0.142	0.139
1.260	0.037	0.326	0.250	0.113
1.262	0.072	0.486	0.486	0.072
1.263	0.016	0.490	0.375	0.131
1.264	0.013	0.323	0.179	0.157
1.267	0.012	0.329	0.178	0.162
1.268	0.004	0.386	0.263	0.127
1.270	0.000	0.494	0.371	0.124

1.271	0.019	0.490	0.385	0.124
1.271	0.009	0.494	0.375	0.129
1.274	0.119	0.198	0.193	0.124
1.277	0.007	0.420	0.254	0.174
1.278	0.125	0.183	0.155	0.152
1.280	0.002	0.415	0.224	0.193
1.281	0.003	0.412	0.219	0.197
1.288	0.007	0.416	0.258	0.166
1.295	0.082	0.286	0.202	0.165
1.300	0.075	0.328	0.256	0.146
1.300	0.081	0.287	0.196	0.173
1.301	0.111	0.317	0.317	0.112
1.302	0.000	0.491	0.252	0.239
1.304	0.080	0.326	0.253	0.152
1.304	0.001	0.492	0.251	0.243
1.304	0.048	0.371	0.258	0.160
1.307	0.079	0.324	0.258	0.145
1.308	0.030	0.431	0.292	0.169
1.308	0.056	0.403	0.326	0.133
1.309	0.073	0.326	0.248	0.151
1.310	0.162	0.258	0.254	0.166
1.310	0.034	0.409	0.282	0.162
1.312	0.029	0.495	0.319	0.205
1.312	0.044	0.373	0.263	0.153
1.312	0.073	0.323	0.247	0.148
1.313	0.042	0.413	0.296	0.159
1.314	0.027	0.436	0.278	0.184
1.314	0.144	0.262	0.249	0.157
1.317	0.031	0.491	0.327	0.196
1.317	0.075	0.319	0.251	0.143
1.318	0.049	0.402	0.317	0.134
1.319	0.043	0.391	0.240	0.194
1.319	0.026	0.490	0.318	0.198
1.320	0.046	0.388	0.235	0.198
1.322	0.031	0.485	0.324	0.192
1.323	0.025	0.495	0.329	0.191
1.324	0.024	0.495	0.327	0.193
1.326	0.023	0.493	0.318	0.197
1.334	0.020	0.499	0.323	0.195
1.337	0.085	0.485	0.411	0.159
1.337	0.107	0.414	0.375	0.146
1.339	0.062	0.497	0.399	0.159
1.340	0.110	0.399	0.367	0.142
1.340	0.097	0.432	0.375	0.154
1.340	0.088	0.426	0.368	0.145
1.340	0.129	0.414	0.406	0.137
1.341	0.108	0.410	0.369	0.148
1.342	0.080	0.489	0.408	0.160
1.342	0.070	0.490	0.397	0.163
1.342	0.147	0.491	0.490	0.147
1.342	0.145	0.493	0.488	0.150
1.343	0.074	0.495	0.408	0.161
1.344	0.101	0.374	0.323	0.152
1.344	0.078	0.465	0.384	0.159
1.346	0.107	0.401	0.370	0.138
1.347	0.073	0.495	0.408	0.159
1.347	0.136	0.495	0.491	0.140
1.347	0.106	0.411	0.370	0.147
1.347	0.066	0.492	0.405	0.154
1.347	0.072	0.466	0.382	0.156
1.348	0.066	0.496	0.400	0.161
1.349	0.115	0.409	0.373	0.151
1.349	0.138	0.493	0.491	0.140
1.351	0.184	0.278	0.276	0.186

1.352	0.098	0.376	0.318	0.156
1.353	0.146	0.490	0.489	0.147
1.353	0.143	0.494	0.492	0.145
1.354	0.141	0.491	0.487	0.145
1.354	0.145	0.489	0.487	0.147
1.355	0.136	0.497	0.490	0.143
1.355	0.139	0.493	0.490	0.142
1.355	0.146	0.498	0.494	0.150
1.356	0.139	0.489	0.489	0.139
1.362	0.141	0.497	0.494	0.144
1.370	0.084	0.436	0.263	0.258
1.371	0.120	0.370	0.246	0.244
1.373	0.122	0.368	0.246	0.244
1.375	0.242	0.273	0.260	0.255
1.376	0.124	0.382	0.284	0.222
1.376	0.135	0.394	0.292	0.237
1.377	0.125	0.379	0.257	0.248
1.377	0.090	0.431	0.267	0.254
1.378	0.077	0.486	0.284	0.279
1.378	0.061	0.492	0.280	0.274
1.382	0.087	0.491	0.295	0.284
1.384	0.065	0.499	0.287	0.277
1.410	0.158	0.491	0.393	0.255
1.411	0.206	0.367	0.323	0.250
1.414	0.209	0.379	0.324	0.264
1.415	0.226	0.384	0.382	0.228
1.415	0.189	0.430	0.367	0.253
1.416	0.188	0.431	0.368	0.252
1.416	0.150	0.490	0.386	0.255
1.418	0.180	0.444	0.372	0.252
1.418	0.181	0.440	0.370	0.250
1.419	0.188	0.433	0.366	0.255
1.419	0.167	0.469	0.376	0.261
1.420	0.159	0.489	0.389	0.258
1.421	0.155	0.494	0.392	0.258
1.422	0.156	0.487	0.390	0.253
1.423	0.253	0.494	0.492	0.256
1.424	0.169	0.459	0.371	0.257
1.424	0.188	0.431	0.372	0.247
1.425	0.159	0.484	0.386	0.257
1.426	0.147	0.495	0.388	0.254
1.426	0.243	0.498	0.494	0.247
1.427	0.248	0.495	0.488	0.256
1.428	0.143	0.496	0.385	0.254
1.433	0.238	0.490	0.488	0.240
1.433	0.252	0.494	0.494	0.252
1.434	0.246	0.490	0.487	0.249
1.434	0.242	0.492	0.481	0.253
1.434	0.244	0.495	0.494	0.245
1.435	0.247	0.492	0.492	0.247
1.435	0.250	0.482	0.482	0.250
1.437	0.251	0.494	0.492	0.252
1.455	0.340	0.371	0.370	0.341
1.461	0.279	0.472	0.376	0.375
1.464	0.271	0.488	0.386	0.373
1.466	0.268	0.477	0.375	0.370
1.467	0.249	0.496	0.374	0.371
1.467	0.285	0.458	0.373	0.370
1.469	0.259	0.492	0.377	0.374
1.470	0.257	0.485	0.376	0.366
1.481	0.368	0.489	0.488	0.368
1.481	0.370	0.493	0.491	0.371
1.481	0.366	0.496	0.495	0.367
1.482	0.365	0.492	0.490	0.367

1.482	0.370	0.490	0.487	0.373
1.483	0.366	0.495	0.491	0.370
1.485	0.367	0.493	0.491	0.370
1.485	0.375	0.489	0.487	0.377
1.486	0.366	0.487	0.484	0.369
1.500	0.482	0.497	0.490	0.489
1.500	0.489	0.494	0.492	0.490
1.500	0.488	0.493	0.491	0.490

TABLE V: Data from Three-Qubit, Mitigated, Simulated Calculations

Eigenvalue	**Degree of Pinning**	n_4	n_5	n_6
1.002	0.000	0.146	0.145	0.000
1.002	0.000	0.016	0.016	0.000
1.003	0.000	0.015	0.015	0.000
1.003	0.000	0.484	0.484	0.000
1.003	0.000	0.365	0.365	0.000
1.003	-0.001	0.000	0.000	0.000
1.004	0.000	0.151	0.151	0.000
1.005	0.000	0.253	0.253	0.000
1.005	0.000	0.073	0.073	0.000
1.005	0.000	0.493	0.493	0.000
1.006	0.000	0.485	0.485	0.000
1.006	0.000	0.065	0.065	0.000
1.006	0.000	0.245	0.245	0.000
1.006	0.000	0.066	0.066	0.000
1.007	0.000	0.254	0.253	0.000
1.007	0.000	0.484	0.484	0.000
1.007	0.000	0.481	0.481	0.000
1.007	0.000	0.492	0.492	0.000
1.007	0.000	0.489	0.489	0.000
1.007	0.000	0.490	0.490	0.000
1.008	0.000	0.373	0.372	0.000
1.009	0.000	0.141	0.141	0.000
1.011	0.000	0.497	0.497	0.000
1.011	0.000	0.017	0.017	0.000
1.012	0.000	0.377	0.377	0.000
1.032	0.001	0.372	0.372	0.001
1.032	0.001	0.032	0.018	0.015
1.033	0.000	0.029	0.015	0.014
1.033	0.001	0.033	0.018	0.016
1.044	0.003	0.082	0.069	0.016
1.058	0.021	0.036	0.034	0.023
1.061	0.002	0.077	0.063	0.016
1.062	0.003	0.382	0.381	0.004
1.062	0.003	0.258	0.258	0.004
1.066	0.001	0.078	0.063	0.016
1.067	0.003	0.078	0.064	0.017
1.067	0.002	0.081	0.067	0.016
1.072	0.015	0.085	0.083	0.017
1.072	0.003	0.081	0.069	0.015
1.077	0.010	0.155	0.154	0.011
1.079	0.005	0.163	0.151	0.017
1.088	0.004	0.159	0.146	0.018
1.089	0.005	0.156	0.144	0.017
1.089	0.007	0.413	0.413	0.008
1.089	0.004	0.157	0.146	0.015
1.090	0.005	0.161	0.147	0.018
1.092	0.018	0.078	0.061	0.035
1.099	0.015	0.082	0.063	0.035
1.099	0.006	0.153	0.140	0.019
1.111	0.008	0.254	0.244	0.018
1.111	0.009	0.263	0.255	0.017

1.111	0.008	0.255	0.247	0.017
1.112	0.013	0.437	0.435	0.014
1.115	0.008	0.127	0.069	0.066
1.115	0.016	0.284	0.282	0.019
1.116	0.008	0.257	0.249	0.016
1.116	0.007	0.254	0.244	0.017
1.116	0.006	0.120	0.081	0.045
1.117	0.008	0.155	0.129	0.034
1.119	0.011	0.123	0.067	0.067
1.120	0.015	0.492	0.491	0.016
1.121	0.001	0.196	0.158	0.039
1.121	0.007	0.127	0.068	0.066
1.122	0.015	0.487	0.482	0.019
1.122	0.016	0.490	0.490	0.016
1.123	0.016	0.486	0.486	0.016
1.123	0.001	0.286	0.263	0.024
1.124	0.012	0.380	0.375	0.016
1.125	0.007	0.125	0.082	0.049
1.125	0.008	0.254	0.245	0.017
1.125	0.014	0.373	0.369	0.017
1.125	0.016	0.490	0.488	0.018
1.126	0.015	0.380	0.376	0.019
1.126	0.018	0.493	0.492	0.020
1.127	0.015	0.486	0.484	0.017
1.127	0.013	0.367	0.363	0.018
1.128	0.014	0.388	0.383	0.018
1.128	0.015	0.491	0.490	0.016
1.128	0.000	0.278	0.254	0.024
1.129	0.016	0.494	0.493	0.017
1.129	0.015	0.493	0.492	0.016
1.129	0.015	0.373	0.371	0.017
1.130	0.016	0.464	0.462	0.018
1.130	0.016	0.486	0.484	0.018
1.130	0.018	0.495	0.494	0.018
1.131	0.012	0.163	0.137	0.037
1.132	0.015	0.495	0.495	0.015
1.132	0.014	0.491	0.490	0.015
1.133	0.007	0.392	0.380	0.018
1.133	0.015	0.490	0.490	0.016
1.133	0.000	0.187	0.156	0.032
1.134	0.005	0.386	0.375	0.015
1.137	0.002	0.407	0.383	0.026
1.137	0.016	0.485	0.484	0.018
1.139	0.017	0.491	0.490	0.017
1.143	0.005	0.255	0.225	0.036
1.143	0.003	0.407	0.390	0.020
1.148	0.065	0.094	0.081	0.079
1.151	0.003	0.252	0.222	0.033
1.152	0.000	0.427	0.403	0.025
1.152	0.000	0.195	0.113	0.082
1.156	0.000	0.379	0.347	0.032
1.156	0.001	0.193	0.114	0.080
1.159	0.001	0.435	0.407	0.029
1.160	0.000	0.470	0.440	0.030
1.160	0.001	0.474	0.441	0.033
1.160	0.004	0.491	0.459	0.036
1.160	0.004	0.495	0.464	0.035
1.161	0.036	0.192	0.190	0.038
1.162	0.006	0.487	0.460	0.033
1.164	0.000	0.318	0.278	0.040
1.165	0.002	0.384	0.351	0.034
1.166	0.005	0.490	0.460	0.035
1.167	0.062	0.130	0.130	0.062
1.168	0.028	0.314	0.313	0.029

1.170	0.017	0.193	0.142	0.068
1.172	0.001	0.317	0.282	0.036
1.175	0.018	0.195	0.146	0.067
1.175	0.017	0.191	0.141	0.066
1.175	0.021	0.198	0.150	0.069
1.177	0.019	0.190	0.143	0.066
1.177	0.017	0.192	0.145	0.063
1.188	0.012	0.255	0.190	0.078
1.189	0.010	0.253	0.195	0.068
1.191	0.001	0.291	0.209	0.083
1.197	0.002	0.246	0.161	0.087
1.197	0.063	0.161	0.145	0.078
1.198	0.069	0.155	0.140	0.084
1.200	0.003	0.254	0.160	0.098
1.201	0.000	0.282	0.202	0.080
1.204	0.006	0.375	0.324	0.057
1.206	0.006	0.369	0.321	0.055
1.208	0.039	0.190	0.123	0.106
1.209	0.030	0.283	0.251	0.062
1.209	0.035	0.192	0.124	0.103
1.212	0.031	0.280	0.248	0.063
1.213	0.015	0.328	0.259	0.083
1.214	0.036	0.289	0.260	0.065
1.214	0.041	0.282	0.253	0.070
1.216	0.069	0.253	0.252	0.071
1.216	0.029	0.286	0.252	0.062
1.218	0.046	0.376	0.375	0.047
1.221	0.035	0.282	0.253	0.064
1.226	0.013	0.328	0.268	0.073
1.229	0.011	0.390	0.317	0.085
1.229	0.005	0.382	0.308	0.080
1.229	0.052	0.254	0.226	0.080
1.230	0.056	0.259	0.233	0.081
1.231	0.062	0.442	0.441	0.063
1.232	0.012	0.431	0.377	0.066
1.232	0.001	0.326	0.195	0.132
1.234	0.068	0.488	0.486	0.070
1.236	0.056	0.494	0.489	0.061
1.236	0.020	0.284	0.178	0.126
1.237	0.016	0.477	0.418	0.076
1.237	0.014	0.443	0.383	0.075
1.237	0.031	0.434	0.392	0.073
1.237	0.057	0.389	0.375	0.071
1.238	0.049	0.378	0.362	0.066
1.238	0.004	0.366	0.270	0.100
1.240	0.017	0.277	0.171	0.124
1.241	0.004	0.377	0.287	0.094
1.241	0.039	0.409	0.374	0.074
1.241	0.066	0.491	0.490	0.066
1.243	0.070	0.487	0.486	0.070
1.243	0.032	0.386	0.332	0.087
1.243	0.001	0.315	0.191	0.125
1.245	0.044	0.250	0.150	0.144
1.245	0.061	0.491	0.490	0.061
1.245	0.045	0.384	0.366	0.064
1.245	0.020	0.489	0.426	0.083
1.245	0.033	0.372	0.322	0.083
1.246	0.024	0.495	0.434	0.086
1.246	0.063	0.494	0.493	0.064
1.246	0.050	0.380	0.367	0.062
1.247	0.037	0.327	0.252	0.112
1.247	0.067	0.492	0.491	0.068
1.248	0.027	0.491	0.441	0.077
1.248	0.068	0.493	0.492	0.070

1.248	0.032	0.414	0.379	0.067
1.249	0.031	0.486	0.436	0.081
1.250	0.002	0.439	0.328	0.113
1.251	0.067	0.494	0.491	0.070
1.251	0.045	0.387	0.368	0.065
1.253	0.065	0.486	0.484	0.067
1.253	0.020	0.463	0.407	0.076
1.253	0.063	0.495	0.492	0.067
1.253	0.022	0.443	0.394	0.070
1.254	0.066	0.492	0.491	0.066
1.254	0.036	0.490	0.438	0.088
1.254	0.047	0.380	0.362	0.065
1.255	0.064	0.495	0.492	0.067
1.255	0.023	0.494	0.438	0.080
1.256	0.041	0.487	0.442	0.086
1.256	0.044	0.258	0.156	0.146
1.257	0.003	0.389	0.262	0.130
1.257	0.020	0.491	0.428	0.083
1.258	0.065	0.495	0.495	0.065
1.258	0.001	0.431	0.314	0.118
1.259	0.040	0.242	0.142	0.139
1.260	0.037	0.326	0.250	0.113
1.262	0.072	0.486	0.486	0.072
1.263	0.016	0.490	0.375	0.131
1.264	0.013	0.323	0.179	0.157
1.267	0.012	0.329	0.178	0.162
1.268	0.004	0.386	0.263	0.127
1.270	0.000	0.494	0.371	0.124
1.271	0.019	0.490	0.385	0.124
1.271	0.009	0.494	0.375	0.129
1.274	0.119	0.198	0.193	0.124
1.277	0.007	0.420	0.254	0.174
1.278	0.125	0.183	0.155	0.152
1.280	0.002	0.415	0.224	0.193
1.281	0.003	0.412	0.219	0.197
1.288	0.007	0.416	0.258	0.166
1.295	0.082	0.286	0.202	0.165
1.300	0.075	0.328	0.256	0.146
1.300	0.081	0.287	0.196	0.173
1.301	0.111	0.317	0.317	0.112
1.302	0.000	0.491	0.252	0.239
1.304	0.080	0.326	0.253	0.152
1.304	0.001	0.492	0.251	0.243
1.304	0.048	0.371	0.258	0.160
1.307	0.079	0.324	0.258	0.145
1.308	0.030	0.431	0.292	0.169
1.308	0.056	0.403	0.326	0.133
1.309	0.073	0.326	0.248	0.151
1.310	0.162	0.258	0.254	0.166
1.310	0.034	0.409	0.282	0.162
1.312	0.029	0.495	0.319	0.205
1.312	0.044	0.373	0.263	0.153
1.312	0.073	0.323	0.247	0.148
1.313	0.042	0.413	0.296	0.159
1.314	0.027	0.436	0.278	0.184
1.314	0.144	0.262	0.249	0.157
1.317	0.031	0.491	0.327	0.196
1.317	0.075	0.319	0.251	0.143
1.318	0.049	0.402	0.317	0.134
1.319	0.043	0.391	0.240	0.194
1.319	0.026	0.490	0.318	0.198
1.320	0.046	0.388	0.235	0.198
1.322	0.031	0.485	0.324	0.192
1.323	0.025	0.495	0.329	0.191

1.324	0.024	0.495	0.327	0.193
1.326	0.023	0.493	0.318	0.197
1.334	0.020	0.499	0.323	0.195
1.337	0.085	0.485	0.411	0.159
1.337	0.107	0.414	0.375	0.146
1.339	0.062	0.497	0.399	0.159
1.340	0.110	0.399	0.367	0.142
1.340	0.097	0.432	0.375	0.154
1.340	0.088	0.426	0.368	0.145
1.340	0.129	0.414	0.406	0.137
1.341	0.108	0.410	0.369	0.148
1.342	0.080	0.489	0.408	0.160
1.342	0.070	0.490	0.397	0.163
1.342	0.147	0.491	0.490	0.147
1.342	0.145	0.493	0.488	0.150
1.343	0.074	0.495	0.408	0.161
1.344	0.101	0.374	0.323	0.152
1.344	0.078	0.465	0.384	0.159
1.346	0.107	0.401	0.370	0.138
1.347	0.073	0.495	0.408	0.159
1.347	0.136	0.495	0.491	0.140
1.347	0.106	0.411	0.370	0.147
1.347	0.066	0.492	0.405	0.154
1.347	0.072	0.466	0.382	0.156
1.348	0.066	0.496	0.400	0.161
1.349	0.115	0.409	0.373	0.151
1.349	0.138	0.493	0.491	0.140
1.351	0.184	0.278	0.276	0.186
1.352	0.098	0.376	0.318	0.156
1.353	0.146	0.490	0.489	0.147
1.353	0.143	0.494	0.492	0.145
1.354	0.141	0.491	0.487	0.145
1.354	0.145	0.489	0.487	0.147
1.355	0.136	0.497	0.490	0.143
1.355	0.139	0.493	0.490	0.142
1.355	0.146	0.498	0.494	0.150
1.356	0.139	0.489	0.489	0.139
1.362	0.141	0.497	0.494	0.144
1.370	0.084	0.436	0.263	0.258
1.371	0.120	0.370	0.246	0.244
1.373	0.122	0.368	0.246	0.244
1.375	0.242	0.273	0.260	0.255
1.376	0.124	0.382	0.284	0.222
1.376	0.135	0.394	0.292	0.237
1.377	0.125	0.379	0.257	0.248
1.377	0.090	0.431	0.267	0.254
1.378	0.077	0.486	0.284	0.279
1.378	0.061	0.492	0.280	0.274
1.382	0.087	0.491	0.295	0.284
1.384	0.065	0.499	0.287	0.277
1.410	0.158	0.491	0.393	0.255
1.411	0.206	0.367	0.323	0.250
1.414	0.209	0.379	0.324	0.264
1.415	0.226	0.384	0.382	0.228
1.415	0.189	0.430	0.367	0.253
1.416	0.188	0.431	0.368	0.252
1.416	0.150	0.490	0.386	0.255
1.418	0.180	0.444	0.372	0.252
1.418	0.181	0.440	0.370	0.250
1.419	0.188	0.433	0.366	0.255
1.419	0.167	0.469	0.376	0.261
1.420	0.159	0.489	0.389	0.258
1.421	0.155	0.494	0.392	0.258
1.422	0.156	0.487	0.390	0.253

1.423	0.253	0.494 0.492 0.256
1.424	0.169	0.459 0.371 0.257
1.424	0.188	0.431 0.372 0.247
1.425	0.159	0.484 0.386 0.257
1.426	0.147	0.495 0.388 0.254
1.426	0.243	0.498 0.494 0.247
1.427	0.248	0.495 0.488 0.256
1.428	0.143	0.496 0.385 0.254
1.433	0.238	0.490 0.488 0.240
1.433	0.252	0.494 0.494 0.252
1.434	0.246	0.490 0.487 0.249
1.434	0.242	0.492 0.481 0.253
1.434	0.244	0.495 0.494 0.245
1.435	0.247	0.492 0.492 0.247
1.435	0.250	0.482 0.482 0.250
1.437	0.251	0.494 0.492 0.252
1.455	0.340	0.371 0.370 0.341
1.461	0.279	0.472 0.376 0.375
1.464	0.271	0.488 0.386 0.373
1.466	0.268	0.477 0.375 0.370
1.467	0.249	0.496 0.374 0.371
1.467	0.285	0.458 0.373 0.370
1.469	0.259	0.492 0.377 0.374
1.470	0.257	0.485 0.376 0.366
1.481	0.368	0.489 0.488 0.368
1.481	0.370	0.493 0.491 0.371
1.481	0.366	0.496 0.495 0.367
1.482	0.365	0.492 0.490 0.367
1.482	0.370	0.490 0.487 0.373
1.483	0.366	0.495 0.491 0.370
1.485	0.367	0.493 0.491 0.370
1.485	0.375	0.489 0.487 0.377
1.486	0.366	0.487 0.484 0.369
1.500	0.482	0.497 0.490 0.489
1.500	0.489	0.494 0.492 0.490
1.500	0.488	0.493 0.491 0.490

TABLE VI: Data from Three-Qubit, Experimental Calculations

Eigenvalue	**Degree of Pinning**	n_4	n_5	n_6
0.893	0.004	0.447	0.368	0.083
0.935	0.028	0.437	0.373	0.092
0.947	0.171	0.440	0.361	0.249
0.964	0.007	0.222	0.208	0.022
0.965	-0.075	0.477	0.378	0.024
0.972	-0.070	0.465	0.369	0.026
0.977	-0.040	0.451	0.383	0.028
0.984	-0.074	0.471	0.372	0.025
0.994	0.099	0.466	0.420	0.145
0.997	-0.011	0.426	0.382	0.033
1.001	-0.012	0.431	0.383	0.036
1.004	0.058	0.237	0.224	0.072
1.009	-0.056	0.454	0.365	0.033
1.014	0.003	0.072	0.054	0.021
1.024	0.020	0.426	0.353	0.093
1.025	0.028	0.074	0.070	0.032
1.035	-0.035	0.448	0.364	0.049
1.040	0.016	0.025	0.024	0.017
1.053	-0.047	0.455	0.365	0.042
1.096	-0.017	0.463	0.385	0.060
1.100	0.026	0.119	0.076	0.069
1.106	0.068	0.426	0.408	0.087
1.119	0.127	0.440	0.347	0.220

1.134	0.007	0.443	0.377	0.073
1.140	0.083	0.424	0.399	0.108
1.141	0.036	0.249	0.210	0.075
1.143	0.298	0.452	0.421	0.330
1.163	0.034	0.440	0.385	0.088
1.166	0.011	0.452	0.371	0.092
1.177	-0.001	0.452	0.374	0.078
1.184	0.048	0.461	0.384	0.126
1.187	0.099	0.247	0.233	0.113
1.208	0.135	0.465	0.428	0.173
1.228	0.078	0.463	0.384	0.157
1.242	0.230	0.427	0.422	0.235
1.257	0.250	0.439	0.418	0.271
1.267	0.112	0.458	0.392	0.178
1.288	0.152	0.456	0.385	0.223
1.290	0.159	0.330	0.251	0.239
1.299	0.184	0.462	0.384	0.261
1.313	0.156	0.479	0.388	0.247
1.316	0.418	0.428	0.428	0.419
1.333	0.230	0.464	0.394	0.300
1.340	0.284	0.470	0.453	0.301
1.342	0.282	0.455	0.395	0.341
1.345	0.321	0.468	0.398	0.390
1.360	0.368	0.470	0.441	0.397
1.372	0.373	0.484	0.465	0.392
1.378	0.362	0.487	0.464	0.385
1.386	0.344	0.491	0.452	0.383

TABLE VII: Data from Three-Qubit, Mitigated, Experimental Calculations

Eigenvalue	**Degree of Pinning**	n_4	n_5	n_6
0.967	0.034	0.434	0.433	0.035
0.972	0.029	0.433	0.430	0.032
0.980	0.014	0.462	0.455	0.021
0.989	0.010	0.022	0.021	0.011
0.991	0.016	0.458	0.454	0.020
0.999	0.021	0.465	0.465	0.022
1.001	0.017	0.233	0.231	0.019
1.002	0.014	0.073	0.071	0.017
1.005	0.027	0.464	0.462	0.029
1.006	0.039	0.450	0.439	0.050
1.007	0.017	0.472	0.469	0.020
1.008	0.005	0.074	0.062	0.017
1.029	0.019	0.456	0.446	0.029
1.031	0.081	0.439	0.425	0.096
1.035	0.065	0.446	0.427	0.084
1.036	0.003	0.244	0.238	0.008
1.070	0.033	0.465	0.460	0.039
1.074	0.094	0.443	0.427	0.110
1.099	0.062	0.452	0.430	0.084
1.112	0.077	0.435	0.425	0.087
1.117	0.009	0.128	0.075	0.063
1.120	0.056	0.459	0.458	0.057
1.134	0.078	0.444	0.432	0.090
1.165	0.059	0.458	0.447	0.070
1.168	0.031	0.261	0.218	0.073
1.194	0.082	0.460	0.451	0.090
1.201	0.063	0.462	0.450	0.075
1.211	0.026	0.271	0.236	0.061
1.221	0.237	0.440	0.416	0.261
1.224	0.105	0.474	0.454	0.125
1.239	0.051	0.482	0.473	0.060

1.245	0.216	0.455 0.424 0.247
1.249	0.280	0.445 0.442 0.283
1.267	0.142	0.473 0.459 0.156
1.309	0.165	0.474 0.459 0.179
1.327	0.106	0.356 0.239 0.223
1.328	0.231	0.442 0.440 0.233
1.329	0.421	0.459 0.454 0.427
1.332	0.210	0.476 0.461 0.224
1.346	0.256	0.473 0.467 0.262
1.354	0.237	0.462 0.450 0.249
1.360	0.432	0.463 0.459 0.436
1.379	0.204	0.481 0.470 0.215
1.383	0.280	0.486 0.463 0.302
1.399	0.331	0.474 0.462 0.343
1.400	0.385	0.473 0.464 0.394
1.414	0.421	0.476 0.457 0.440
1.435	0.444	0.462 0.460 0.447
1.436	0.453	0.477 0.467 0.464
1.438	0.450	0.470 0.469 0.451

IV. BOSONIC AND FERMIONIC STATISTICS

A single qubit—the analogue to the classical bit on a quantum device—can be represented according to $\cos\left(\frac{\theta}{2}\right)|0\rangle + e^{i\phi}\sin\left(\frac{\theta}{2}\right)|1\rangle$, which can be pictorially depicted by the image of the Bloch sphere shown. The quantum bit is hence

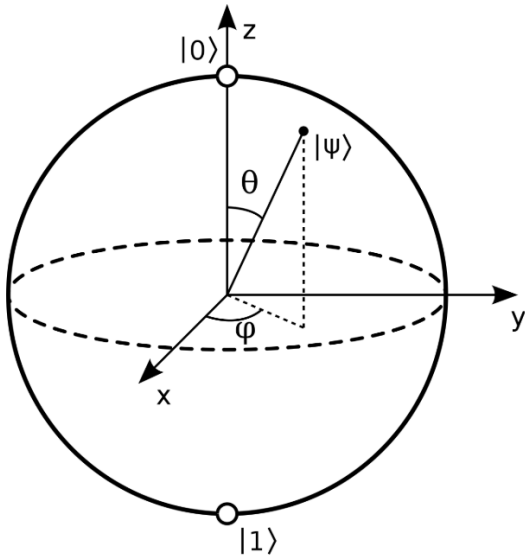

a linear combination of the classical bit states, $|0\rangle$ and $|1\rangle$. The classical bit states are represented in vector form as follows.

$$|0\rangle = \begin{pmatrix} 1 \\ 0 \end{pmatrix}$$

$$|1\rangle = \begin{pmatrix} 0 \\ 1 \end{pmatrix}$$

A. One Particle in Two Orbitals

As described in the main text, we view each qubit as being composed of one particle in two particle-hole paired orbitals. As such, if qubit i exists in the $|0\rangle$ state, a particle exists in the orbital which we denote as $i,0$ and a hole exists in the orbital denoted as $i,1$. Similarly, if qubit i exists in the $|1\rangle$ state, a particle exists in the orbital which we denote as $i,1$ and a hole exists in the orbital denoted as $i,0$. Below, we apply bosonic and fermionic statistics for such a qubit interpretation.

1. General Bosonic Statistics

Bosons must obey the commutation relationship,

$$[\hat{b}_i, \hat{b}_j^\dagger] = \hat{b}_i\hat{b}_j^\dagger - \hat{b}_j^\dagger\hat{b}_i = \delta_j^i,$$

where $\hat{b}_i^\dagger$ and $\hat{b}_i$ are bosonic creation and annihilation operators for orbital i such they act on a wavefunction as shown below.

$$\hat{b}_i|i \wedge \psi\rangle = \sqrt{n}|\psi\rangle$$

$$\hat{b}_i^\dagger|\psi\rangle = \sqrt{n+1}|i \wedge \psi\rangle$$

The bosonic commutation relationship can be proven as follows for the case of $i = j$ for qubit p—which exists in a linear combination of $|0\rangle$ and $|1\rangle$, i.e. $|\psi\rangle_p = \cos\left(\frac{\theta}{2}\right)|0\rangle + e^{i\phi}\sin\left(\frac{\theta}{2}\right)|1\rangle$—as can be seen by

$$\hat{b}_{p,0}\hat{b}_{p,0}^\dagger - \hat{b}_{p,0}^\dagger\hat{b}_{p,0} = [2 \times P(|0\rangle) + P(|1\rangle)] - P(|0\rangle) = P(|1\rangle) + P(|0\rangle) = \delta_{p,0}^{p,0} = 1$$

and

$$\hat{b}_{p,1}\hat{b}_{p,1}^\dagger - \hat{b}_{p,1}^\dagger\hat{b}_{p,1} = [2 \times P(|1\rangle) + P(|0\rangle)] - P(|1\rangle) = P(|0\rangle) + P(|1\rangle) = \delta_{p,1}^{p,1} = 1$$

where $P(|0\rangle)$ and $P(|1\rangle)$ are the probabilities of the qubit being in the $|0\rangle$ and $|1\rangle$ respectively.

When $i \neq j$, this bosonic commutation yields the following two relationships, which must be obeyed by bosons.

$$\hat{b}_{p,0}\hat{b}_{p,1}^\dagger - \hat{b}_{p,1}^\dagger\hat{b}_{p,0} = \delta_{p,1}^{p,0} = 0 \Rightarrow \hat{b}_{p,0}\hat{b}_{p,1}^\dagger = +\hat{b}_{p,1}^\dagger\hat{b}_{p,0}$$

$$\hat{b}_{p,1}\hat{b}_{p,0}^\dagger - \hat{b}_{p,0}^\dagger\hat{b}_{p,1} = \delta_{p,0}^{p,1} = 0 \Rightarrow \hat{b}_{p,1}\hat{b}_{p,0}^\dagger = +\hat{b}_{p,0}^\dagger\hat{b}_{p,1}$$

2. General Fermionic Statistics

Fermions must obey the anticommutation relationship

$$\{\hat{a}_i, \hat{a}_j^\dagger\} = \hat{a}_i\hat{a}_j^\dagger + \hat{a}_j^\dagger\hat{a}_i = \delta_j^i$$

where $\hat{a}_i^\dagger$ and $\hat{a}_i^\dagger$ are fermionic creation and annihilation operators for orbital i.

The fermionic anticommutation relationship can be proven as follows for the case of $i = j$ for qubit p—which exists in a linear combination of $|0\rangle$ and $|1\rangle$, i.e. $|\psi\rangle_p = \cos\left(\frac{\theta}{2}\right)|0\rangle + e^{i\phi}\sin\left(\frac{\theta}{2}\right)|1\rangle$—as can be seen by

$$\hat{a}_{p,0}\hat{a}_{p,0}^\dagger + \hat{a}_{p,0}^\dagger\hat{a}_{p,0} = P(|1\rangle) + P(|0\rangle) = \delta_{p,0}^{p,0} = 1$$

and

$$\hat{a}_{p,1}\hat{a}_{p,1}^\dagger + \hat{a}_{p,1}^\dagger\hat{a}_{p,1} = P(|0\rangle) + P(|1\rangle) = \delta_{p,1}^{p,1} = 1.$$

When $i \neq j$, this fermionic anticommutation yields the following two relationships, which must be obeyed by

fermions.

$$\hat{a}_{p,0}\hat{a}^{\dagger}_{p,1} + \hat{a}^{\dagger}_{p,1}\hat{a}_{p,0} = \delta^{p,0}_{p,1} = 0 \Rightarrow \hat{a}_{p,0}\hat{a}^{\dagger}_{p,1} = -\hat{a}^{\dagger}_{p,1}\hat{a}_{p,0}$$

$$\hat{a}_{p,1}\hat{a}^{\dagger}_{p,0} + \hat{a}^{\dagger}_{p,0}\hat{a}_{p,1} = \delta^{p,1}_{p,0} = 0 \Rightarrow \hat{a}_{p,1}\hat{a}^{\dagger}_{p,0} = -\hat{a}^{\dagger}_{p,0}\hat{a}_{p,1}$$

3. The Bosonic Qubit

In order to establish when a given qubit can be described as bosonic, we first have to determine when it satisfies the bosonic statistics from above. This can be done by representing the eight possible one-qubit, two-term expectation values as linear combinations of expectation values of the Pauli matrices for the specified qubit. Let's first look at the four previously-established 1-RDM terms (see the Methods section in the main paper).

	$\hat{b}_{p,0}$	$\hat{b}_{p,1}$
$\hat{b}^{\dagger}_{p,0}$	$\hat{b}^{\dagger}_{p,0}\hat{b}_{p,0}$	$\hat{b}^{\dagger}_{p,0}\hat{b}_{p,1}$
$\hat{b}^{\dagger}_{p,1}$	$\hat{b}^{\dagger}_{p,1}\hat{b}_{p,0}$	$\hat{b}^{\dagger}_{p,1}\hat{b}_{p,1}$

These four terms are given by the following four equations and are identical for fermionic and bosonic creation and annihilation operators.

$$\hat{b}^{\dagger}_{p,0}\hat{b}_{p,1} = \begin{pmatrix} 0 & 1 \\ 0 & 0 \end{pmatrix} = \frac{1}{2}\left(X_p + iY_p\right)$$

$$\hat{b}^{\dagger}_{p,1}\hat{b}_{p,0} = \begin{pmatrix} 0 & 0 \\ 1 & 0 \end{pmatrix} = \frac{1}{2}\left(X_p - iY_p\right)$$

$$\hat{b}^{\dagger}_{p,0}\hat{b}_{p,0} = \begin{pmatrix} 1 & 0 \\ 0 & 0 \end{pmatrix} = \frac{1}{2}\left(\hat{I} + Z_p\right)$$

$$\hat{b}^{\dagger}_{p,1}\hat{b}_{p,1} = \begin{pmatrix} 0 & 0 \\ 0 & 1 \end{pmatrix} = \frac{1}{2}\left(\hat{I} - Z_p\right)$$

Now, let's compare these terms with those from the matrix composed as follows.

	$\hat{b}^{\dagger}_{p,0}$	$\hat{b}^{\dagger}_{p,1}$
$\hat{b}_{p,0}$	$\hat{b}_{p,0}\hat{b}^{\dagger}_{p,0}$	$\hat{b}_{p,0}\hat{b}^{\dagger}_{p,1}$
$\hat{b}_{p,1}$	$\hat{b}_{p,1}\hat{b}^{\dagger}_{p,0}$	$\hat{b}_{p,1}\hat{b}^{\dagger}_{p,1}$

These four terms are given by the following four equations. Note that two of these differ from their fermionic counterparts (see below) due to the prefactors associated with bosonic creation and annihilation operatures derived from the fact that more than one boson can be created in a given orbital.

$$\hat{b}_{p,0}\hat{b}^{\dagger}_{p,1} = \begin{pmatrix} 0 & 0 \\ 1 & 0 \end{pmatrix} = \frac{1}{2}\left(X_p - iY_p\right) = \hat{b}^{\dagger}_{p,1}\hat{b}_{p,0}$$

$$\hat{b}_{p,1}\hat{b}^{\dagger}_{p,0} = \begin{pmatrix} 0 & 1 \\ 0 & 0 \end{pmatrix} = \frac{1}{2}\left(X_p + iY_p\right) = \hat{b}^{\dagger}_{p,0}\hat{b}_{p,1}$$

$$\hat{b}_{p,0}\hat{b}^{\dagger}_{p,0} = \begin{pmatrix} 2 & 0 \\ 0 & 1 \end{pmatrix} = \frac{1}{2}\left(3\hat{I} + Z_p\right)$$

$$\hat{b}_{p,1}\hat{b}_{p,1}^{\dagger} = \begin{pmatrix} 1 & 0 \\ 0 & 2 \end{pmatrix} = \frac{1}{2}\left(3\hat{I} - Z_p\right)$$

As can be seen from the above, $\hat{b}_{p,0}\hat{b}_{p,1}^{\dagger} = \hat{b}_{p,1}^{\dagger}\hat{b}_{p,0}$ are $\hat{b}_{p,1}\hat{b}_{p,0}^{\dagger} = \hat{b}_{p,0}^{\dagger}\hat{b}_{p,1}$ are always true, which always satisfies the bosonic commutation relationship. **Hence, bosonic statistics are satisfied by all values of θ and ϕ** and no constraints on the preparations are necessary in order to represent bosons using these creation and annihilation operators.

4. The Fermionic Qubit

In order to establish when a given qubit can be described as fermionic, we first have to determine when it satisfies the fermionic statistics from above. This can be done in a similar manner to that shown for bosonic qubits above. Specifically, let us first look at the four previously-established 1-RDM terms.

	$\hat{a}_{p,0}$	$\hat{a}_{p,1}$
$\hat{a}_{p,0}^{\dagger}$	$\hat{a}_{p,0}^{\dagger}\hat{a}_{p,0}$	$\hat{a}_{p,0}^{\dagger}\hat{a}_{p,1}$
$\hat{a}_{p,1}^{\dagger}$	$\hat{a}_{p,1}^{\dagger}\hat{a}_{p,0}$	$\hat{a}_{p,1}^{\dagger}\hat{a}_{p,1}$

These four terms are given by the following four equations and are identical for fermionic and bosonic creation and annihilation operators.

$$\hat{a}_{p,0}^{\dagger}\hat{a}_{p,1} = \begin{pmatrix} 0 & 1 \\ 0 & 0 \end{pmatrix} = \frac{1}{2}\left(X_p + iY_p\right)$$

$$\hat{a}_{p,1}^{\dagger}\hat{a}_{p,0} = \begin{pmatrix} 0 & 0 \\ 1 & 0 \end{pmatrix} = \frac{1}{2}\left(X_p - iY_p\right)$$

$$\hat{a}_{p,0}^{\dagger}\hat{a}_{p,0} = \begin{pmatrix} 1 & 0 \\ 0 & 0 \end{pmatrix} = \frac{1}{2}\left(\hat{I} + Z_p\right)$$

$$\hat{a}_{p,1}^{\dagger}\hat{a}_{p,1} = \begin{pmatrix} 0 & 0 \\ 0 & 1 \end{pmatrix} = \frac{1}{2}\left(\hat{I} - Z_p\right)$$

Now, let's compare with the terms from the matrix composed as follows.

	$\hat{a}_{p,0}^{\dagger}$	$\hat{a}_{p,1}^{\dagger}$
$\hat{a}_{p,0}$	$\hat{a}_{p,0}\hat{a}_{p,0}^{\dagger}$	$\hat{a}_{p,0}\hat{a}_{p,1}^{\dagger}$
$\hat{a}_{p,1}$	$\hat{a}_{p,1}\hat{a}_{p,0}^{\dagger}$	$\hat{a}_{p,1}\hat{a}_{p,1}^{\dagger}$

These four terms are given by the following four equations.

$$\hat{a}_{p,0}\hat{a}_{p,1}^{\dagger} = \begin{pmatrix} 0 & 0 \\ 1 & 0 \end{pmatrix} = \frac{1}{2}\left(X_p - iY_p\right) = \hat{a}_{p,1}^{\dagger}\hat{a}_{p,0}$$

$$\hat{a}_{p,1}\hat{a}_{p,0}^{\dagger} = \begin{pmatrix} 0 & 1 \\ 0 & 0 \end{pmatrix} = \frac{1}{2}\left(X_p + iY_p\right) = \hat{a}_{p,0}^{\dagger}\hat{a}_{p,1}$$

$$\hat{a}_{p,0}\hat{a}_{p,0}^{\dagger} = \begin{pmatrix} 0 & 0 \\ 0 & 1 \end{pmatrix} = \frac{1}{2}\left(\hat{I} - Z_p\right) = \hat{a}_{p,1}^{\dagger}\hat{a}_{p,1}$$

$$\hat{a}_{p,1}\hat{a}_{p,1}^{\dagger} = \begin{pmatrix} 1 & 0 \\ 0 & 0 \end{pmatrix} = \frac{1}{2}\left(\hat{I} + Z_p\right) = \hat{a}_{p,0}^{\dagger}\hat{a}_{p,0}$$

Note that from the above, $\hat{a}_{p,0}\hat{a}_{p,1}^{\dagger} = \hat{a}_{p,1}^{\dagger}\hat{a}_{p,0}$ and $\hat{a}_{p,1}\hat{a}_{p,0}^{\dagger} = \hat{a}_{p,0}^{\dagger}\hat{a}_{p,1}$; however, for fermionic statistics, $\hat{a}_{p,0}\hat{a}_{p,1}^{\dagger} = -\hat{a}_{p,1}^{\dagger}\hat{a}_{p,0}$ and $\hat{a}_{p,1}\hat{a}_{p,0}^{\dagger} = -\hat{a}_{p,0}^{\dagger}\hat{a}_{p,1}$ must hold. For this to be resolved, we must have $\hat{a}_{p,0}\hat{a}_{p,1}^{\dagger} = \hat{a}_{p,1}^{\dagger}\hat{a}_{p,0} = 0$ or, equivalently,

$$\mathbf{X_p} = \mathbf{Y_p} = \mathbf{0}$$

In order to represent fermions as particles in this interpretation of qubits and satisfy anticommutation relations, the expectation values of $\hat{a}_{p,0}\hat{a}_{p,1}^{\dagger}$ and $\hat{a}_{p,1}^{\dagger}\hat{a}_{p,0}$ must be zero. As such, the one-qubit expectation values of the X and Y Pauli matrices—which can be directly probed on a quantum device—must be zero for all of our preparations. This has been verified through simulation for both preparations—the minimalistic, scanning approach for three qubits described in Equation (10) and the GHZ state preparation described in Equation (13). For the minimalistic, scanning approach, the simulated expectation values for the Pauli X and Y matrices were in the following ranges: [-0.02, 0.02] and [-0.02, 0.02], respectively. The corresponding expectation value for the Pauli Z matrix for these simulations ranged from -0.03 to 1. Similarly, the range for expectation values for the Pauli X and Pauli Y matrices for simulated GHZ states from 3 to 53 qubits was [-0.03, 0.03] and [-0.04, 0.04] respectively. Note that the expectation value of the Pauli Z matrix for these simulations also centered around zero ([-0.03, 0.03]) as the probability of a given qubit being in the $|0\rangle$ or the $|1\rangle$ state were roughly equivalent.

V. ERRORS ON QUANTUM COMPUTERS

Quantum computation has promised to revolutionize the future of technology since the 1980s, yet due to the extreme difficulty in engineering, building, and coding such devices resulting in errors including readout errors, gate noise, and quantum state decoherence, the promise as of yet remains unrealized [6]. Quantum algorithms have historically assumed systems composed of perfect qubits able to be prepared in any desired state and manipulated with complete precision. While physical systems able to act as higher-quality qubit systems are continually being developed, these physical qubits will not be entirely devoid of imperfections in the near future and hence are too imprecise to act as so-called perfect "logical qubits" in near-term quantum devices [7]. Therefore, current quantum computing techniques rely on being able to quantify the error of quantum devices as well as developing techniques to correct for such errors. A description of the types and causes of quantum device errors as well as a brief review of error measurement and mitigation is conducted in the following sections.

A. Types and Causes of Quantum Device Error

In order for a physical system to act as a logical qubit, each qubit system needs to be kept in perfect isolation from external interferences in order to maintain coherence while remaining able to strongly interact with the adjacent qubits on the device in order to allow for information processing. Additionally, the isolated qubit system needs to be able to be externally controlled to allow for state preparation and able to be measured by an external probe to allow for results to be obtained in a readable format [8]. Currently, this seemingly contradictory set of criteria is imperfectly realized, leading to three main types of errors that contribute to the deviation of physical qubits from logical qubits: gate noise, readout noise, and decoherence. Note that in the context of quantum computation the term"noise" is used to refer to imperfections in control of physical qubits [8].

Quantum gates which act on quantum states are operations on a quantum device that correspond to applying a unitary matrix (U) to the vector representation ($|\Psi\rangle$) of quantum states [9]. Multi-qubit quantum gates—the gates prone to the highest rates of error—are well-controlled entangling operations acting on pairs of qubits [8]. For a quantum gate corresponding to a unitary matrix U, a quantum gate error refers to the situation in which the resultant quantum state deviates from $U|\Psi\rangle$. There are two types of gate error—coherent and incoherent gate errors. Coherent gate errors refer to errors that preserve the purity of the input state, i.e. those in which the error can be viewed as a perturbed unitary operation $|\Psi\rangle \rightarrow \tilde{U}|\Psi\rangle$ where $\tilde{U} \neq U$ and are caused by imprecisely-calibrated control of the qubits [9]. Incoherent gate errors, on the other hand, are those that do not preserve the purity of the input state; these errors are caused by imperfect isolation of the qubits from their environment such that the quantum system coevolves with the external degrees of freedom to which it couples [9]. While coherent gate errors can theoretically be decreased by more-precisely calibrating the controls, either a more-isolated quantum device or a robust error-mitigation method is

necessary for decreasing the incoherent gate errors [9]. In general, limiting the number of gates applied—and hence decreasing the gate errors—is optimal for best measurements on quantum devices.

The term readout error refers to transmission line noise that makes the $|0\rangle$ state appear to be the $|1\rangle$ state to a measurement or vice versa. One type of readout error, often referred to as a classical readout bit-flip error, is caused by the probability distributions of the measured physical quantities that correspond to measurement of the $|0\rangle$ and $|1\rangle$ states overlapping, causing a small probability of measuring the opposite value [9, 10]. Additionally, another type of readout error, often referred to as a T1-readout error, is caused by the qubit relaxing/decaying during readout, causing a $|1\rangle$ state to be registered as $|0\rangle$ [9, 10]. Classical readout bip-flip noise can be limited by better-tailoring the optimal readout pulses and/or amplifying the readout signal, while T1-readout error is typically reduced by decreasing the readout pulses relative to the decoherence time (see the following paragraph) [9].

Quantum states are inherently delicate with interactions with external systems often causing the degradation of the quantum state, which is called decoherence [11]. Decoherence is a result of the system interacting with its environment through such means as vibrations, temperature fluctuations, electromagnetic waves, etc., and it destroys the exotic quantum properties of quantum devices [6]. Additionally, the probability of decoherence is known to increase with the size (N) of the qubit state, making larger-scale quantum computations more difficult [8, 11]. While coherence times will likely continue to increase as qubit systems become more and more isolated from their environments, it is likely impossible to completely eliminate quantum decoherence.

B. Measurement of Quantum Device Error

In order to enumerate the amount of error inherent to a quantum device, one must determine the readout error, single-qubit unitary gate (U2) error, and a CNOT error rate. Determination of the readout error is accomplished in a rather straightforward manner where a large number of experiments are prepared with the qubit known to be in either the $|0\rangle$ state or the $|1\rangle$ state with immediate measurement after the preparation. The average value of the percentage of $|1\rangle$ states with a $|1\rangle \rightarrow |0\rangle$ error and the percentage of $|0\rangle$ states with a $|0\rangle \rightarrow |1\rangle$ error is reported to be the readout error of the qubit probed [12].

A single qubit ($U2$) error rate is determined via a scalable randomized benchmarking protocol [13]. In this methodology, a sequence of Clifford gates are applied to a given qubit in order to instigate a random walk along points of the Bloch sphere originating at and returning to the $|0\rangle$ state. As the number of Clifford gates is increased in the walk, the probability of the qubit returning to the original $|0\rangle$ state decreases in an exponential manner, eventually saturating at 50%, indicating pure randomness. The $U2$ value is extrapolated from the fit to the exponential decay in probability [12, 13]. Two-qubit (CNOT) gate error rates are obtained in a similar randomized benchmarking technique, replacing the single-qubit Clifford gates with two-qubit analogues [12, 13].

The decoherence times—$T1$, the relaxation time, and $T2$, the dephasing times—are also reported as a measure of the "noise" of a quantum device. These values are determined through by measuring the time it takes to decay from an initial state ($|1\rangle$ or $\frac{1}{\sqrt{2}}(|0\rangle - |1\rangle)$) to a final state ($|0\rangle$ or $\frac{1}{\sqrt{2}}(|0\rangle + |1\rangle)$) and fitting to the obtained exponential decay [14]. Note that the error introduced by relatively short decoherence times currently far outweigh the errors introduced by readout and gate noise [15].

The above metrics, however, fail to account for errors caused by interactions with spectator qubits and hence can not accurately be used to naïvely estimate the error of a given measurement or set of measurements on a quantum device. IBM has introduced a single-number metric—called quantum volume—meant to encapsulate the error of a quantum computer in a single value to better account for simultaneous all-qubit interactions; however, while quantum volume allows for easy comparison between devices [16], it does not allow for direct calculation of error given the quantum volume value.

C. Mitigation of Quantum Device Error

As described in great detail above, near-term quantum computers will likely continue to have relatively high levels of noise. As such, developing methodologies to either correct for these errors or minimize the errors employed in a given algorithm are necessary to employ quantum devices for the foreseeable future. A quantum variation of the classical repetition code for error correction [17] and the use of linear algebra which gathers information from basis state computations to define a matrix to be used to "project" noisy results to error-mitigated results [7] are traditionally employed to minimize the effects of error. Unfortunately, there is a large computational cost to implementing quantum error correction techniques—namely that the large number of qubits or circuits consumed by the implementation of a quantum error correction scheme leave relatively few qubits available for actual computation and/or are too computationally-expensive for high-qubit mitigation [6, 8].

VI. CONFIDENCE INTERVALS FOR GHZ STATE COMPUTATIONS

In order to establish that the λ_G values obtained from post-measurement computation for a given preparation on a specific quantum computer are consistent between measurements, multiple trials were conducted, and confidence intervals for the resultant samples were calculated according to the methodology described in Sec. VI A. First the optimal number of trials must be established for use in computing the confidence intervals. Ideally, the number of trials will be large enough to accurately obtain the average λ_G value for a given computer and number of qubits but small enough to limit computational expense. To determine the ideal sample size, the several sample sizes for the most-complex computation (that for 53-qubits) were used to establish 95% confidence intervals and these computations were compared.

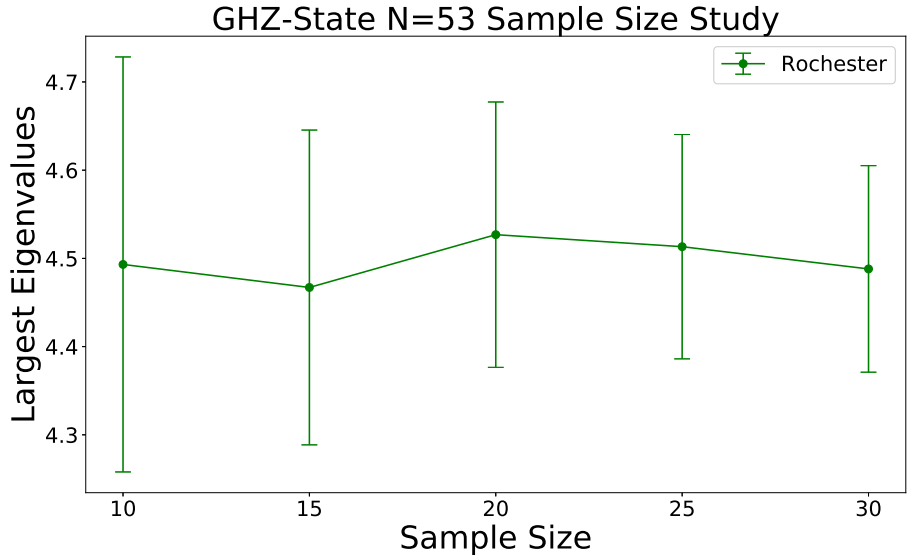

FIG. 2: **Comparison of 95% Confidence Intervals for 53-Qubit Computed λ_G Values on Rochester for Variable Sample Sizes.** The 95% confidence intervals for computed 53-qubit λ_G values obtained from the Rochester 53-qubit IBM Quantum Experience device for the following sample sizes: n=10, 15, 20, 25, 30. Confidence intervals are calculated according to the methodology described in Sec. VI A.

As can be seen in Fig. 2—in which the 95% confidence intervals for the λ_G of 53-qubit GHZ state preparation for differing numbers of trials are shown—, the spread of the confidence interval was relatively small—roughly only five percent of the average value for a sample size of thirty. This indicates that the average value associated with this confidence interval can be interpreted as a characteristic λ_G value associated with the computer (Rochester) and the number of qubits ($N = 53$) probed. Additionally, the average value of λ_G does not seem vary to a significant degree between the sample sizes tested even for this relatively sizeable preparation involving the largest available number of qubits. As such, to minimize computational expense, for the determination of other confidence intervals, a sample size of ten will be utilized.

The 95% confidence intervals for the λ_G values for $N = 3, 4, 5$ for simulation and several different quantum devices are shown for the GHZ state in Fig. VI . As can be seen, despite identical preparations and post-measurement analysis, the character of exciton condensation (λ_G) differ to a statistically-significant degree between computers, likely due to the differing errors associated with each device. However, even for Rochester—the device prone to the largest errors as can be seen from Table III—the confidence intervals are relatively small, which indicates that the λ_G for each individual trial does not vary to an extreme degree (at least for sequential experiments).

A. Determination of Confidence Intervals

Measurement of the signature of exciton condensation (λ_G) on a given quantum device appears to yield results consistent with a normal distribution. Additionally, due to computational expense, the number of trials (n) for the determination of a given λ_G were relatively low ($n \leq 30$), meaning that both the population average (μ) and the

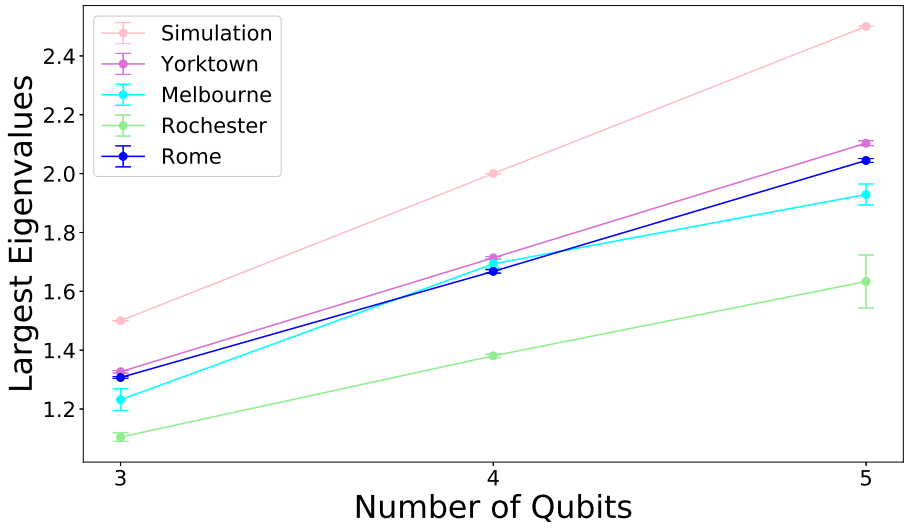

FIG. 3: **Comparison of λ_G Values for Various Devices.** The largest eigenvalue of the unmitigated, experimental ${}^2\tilde{G}$ matrix for experiments of N qubits for the GHZ State are shown for simulations (pink) and experiments on the Yorktown 5-qubits IBM Quantum Experience device (violet), the Melbourne 15-qubit IBM Quantum Experience device (teal), the Rochester 53-qubit IBM Quantum Experience device (lime green), and the Rome 5-qubit IBM Quantum Experience device (blue). Confidence intervals are calculated according to the methodology described in Sec. VI A.

population standard deviation (σ) are unknown. Confidence intervals were hence obtained through use of a family of probability distributions called t distributions. When the mean and standard deviation of a given sample of size n is $\overline{x}$ and s, respectively, then a random variable is defined to be

$$T = \frac{\overline{x} - \mu}{x/\sqrt{n}}. \tag{1}$$

This random variable has a corresponding t_ν distribution with $\nu = n - 1$ degrees of freedom. Each of these t_ν distributions is bell-shaped, centered at zero, and has a greater spread than the normal z distribution. As the number of trials (and hence degrees of freedom) increases, the spread of the t_ν distribution decreases to the point that when $\nu \to \infty$, the t_∞ distribution approaches the normal z distribution. If $t_{\alpha,\nu}$ is defined to be the number on the measurement axis of the t_ν distribution to the right of which the area under the curve is α, then the $100(1-\alpha)\%$ confidence interval for the population average (μ) is given by

$$\left(\overline{x} - t_{\alpha/2,\mu} \cdot \frac{s}{\sqrt{n}}, \overline{x} + t_{\alpha/2,\mu} \cdot \frac{s}{\sqrt{n}}\right) \tag{2}$$

or, equivalently $\overline{x} \pm t_{\alpha/2,\mu} \cdot \frac{s}{\sqrt{n}}$ [18].

VII. SIMULATION AND EXPERIMENTATION FOR VARIOUS TEST CASES

In order to solidify intuition regarding our methodology, we have supplied various test cases in the following sections. Specifically, we supply information regarding a state with no entanglement ($|+\rangle^{\otimes N}$), a statistical mixture ($\frac{1}{2}|0\rangle^{\otimes N}\langle 0|^{\otimes N} + \frac{1}{2}|1\rangle^{\otimes N}\langle 1|^{\otimes N}$), $\frac{N}{2}$ independent two-qubit Bell states in overall N-qubit systems, and—finally—a state demonstrating islands of condensation through construction of $\frac{N}{6}$ independent six-qubit GHZ states in overall N-qubit systems. In the first three examples, we don't expect exciton condensation to be observed as—although the two orbitals corresponding to each qubit i (orbitals $i, 0$ and $i, 1$) are particle-hole paired—these preparations do not entangle the qubits. For the final example of $\frac{N}{6}$ independent six-qubit GHZ states, we expect there to be $\frac{N}{6}$ large eigenvalues of the particle-hole reduced density matrix (RDM)—i.e. $\frac{N}{6}$ λ values exceeding one—as $\frac{N}{6}$ entangled subsystems of qubits are prepared.

A. No Entanglement: $|+\rangle^{\otimes N}$

The $|+\rangle^{\otimes N}$ state for an N-qubit system was prepared by transforming each qubit—initially in the $|0\rangle$ state—to $|+\rangle = \frac{1}{\sqrt{2}}[|0\rangle + |1\rangle]$ through the application of a Hadamard gate. This process is described by

$$|+\rangle^{\otimes N} = H_{N-1} \cdots H_1 H_0 |0\rangle^{\otimes N} \tag{3}$$

where H_i is a Hadamard gate on the i^{th} qubit and $|0\rangle^{\otimes N}$ represents the initial all-zero state. The results for the $|+\rangle^{\otimes N}$ state for simulation and experimentation on IBM's Quantum Experience Yorktown (ibmqx2) device for $N = 3, 4, 5$ are shown in Table VIII. As was expected from the lack of qubit entanglement of the preparation of this state, no eigenvalues significantly exceeding one were observed.

N	Simulation	Yorktown
3	1.00	1.02
4	1.01	1.02
5	1.01	1.02

TABLE VIII: Simulated and non-mitigated, experimental λ_G values for the $|+\rangle^{\otimes N}$ state where $N = 3, 4$, and 5 qubits. Experiments were conducted on IBM's Quantum Experience Yorktown (ibmqx2) device.

B. Statistical Mixture: $\frac{1}{2}|0\rangle^{\otimes N}\langle 0|^{\otimes N} + \frac{1}{2}|1\rangle^{\otimes N}\langle 1|^{\otimes N}$

The statistical mixture of equal proportions of the $|0\rangle^{\otimes N}\langle 0|^{\otimes N}$ and $|1\rangle^{\otimes N}\langle 1|^{\otimes N}$ states were probed by first constructing the modified particle-hole RDM ($^2\tilde{G}$) matrix for the $|0\rangle^{\otimes N}$ initial state and the $|1\rangle^{\otimes N}$ state—prepared by

$$|1\rangle^{\otimes N} = X_{N-1} \cdots X_1 X_0 |0\rangle^{\otimes N} \tag{4}$$

where X_i is the X-gate for the i^{th} qubit—, adding these RDM scaled by a factor of $\frac{1}{2}$, and obtaining the eigenvalues of the resultant average modified particle-hole RDM. The results for the these statistical mixtures for simulation and experimentation on IBM's Quantum Experience Yorktown (ibmqx2) device for $N = 3, 4, 5$ are shown in Table IX. As was expected from the lack of qubit entanglement of the preparation of this state, no eigenvalues significantly exceeding one were observed.

N	Simulation	Yorktown
3	0.51	0.55
4	0.51	0.55
5	0.51	0.55

TABLE IX: Simulated and non-mitigated, experimental λ_G values for the $\frac{1}{2}|0\rangle^{\otimes N}\langle 0|^{\otimes N} + \frac{1}{2}|1\rangle^{\otimes N}\langle 1|^{\otimes N}$ state where $N = 3, 4$, and 5 qubits. Experiments were conducted on IBM's Quantum Experience Yorktown (ibmqx2) device.

C. $\frac{N}{2}$ Independent Two-Qubit Bell States in Overall N-Qubit Systems

Two different Bell states were used to construct overall N-qubit systems consisting of $\frac{N}{2}$ independent two-qubit Bell states: specifically, $|\phi^+\rangle = \frac{1}{\sqrt{2}}[|00\rangle + |11\rangle]$ and $|\psi^+\rangle = \frac{1}{\sqrt{2}}[|01\rangle + |10\rangle]$. These two-qubit Bell states can be constructed between qubits i and j through use of the following preparations:

$$|\phi^+\rangle = C_i^j H_i |00\rangle \tag{5}$$

and

$$|\psi^+\rangle = X_j |\phi^+\rangle = X_j C_i^j H_i |00\rangle \tag{6}$$

where C_i^j is a CNOT gate with control qubit i and target qubit j. For each (even) number of qubits, N, three systems were constructed: one composed of $\frac{N}{2}$ independent $|\phi^+\rangle$ states, one composed of $\frac{N}{2}$ independent $|\psi^+\rangle$ states, and one composed of alternating $|\phi^+\rangle$ and $|\psi^+\rangle$ states in the following order $|\phi^+\psi^+\phi^+\psi^+\phi^+\cdots\rangle$. These states were constructed by applying the preparations given in Eqs. (5) and (6) to the pairs of qubits composing the overall N-qubit systems. For example, for the $N = 6$ $|\phi^+\psi^+\phi^+\rangle$ system, Eq. (5) was applied to qubits-pairs 0/1 and 4/5, and Eq. (6) was applied to the 2/3 qubit pair. The results for the these composite states for simulation and experimentation on IBM's Quantum Experience Melbourne (ibmq_16_melbourne) device for $N = 4, 6, 8, 10$ are shown in Table X. For the most part, the results align with our intuition in that only one experiment demonstrated an eigenvalue significantly above one. This one outlier—the $N = 10$ $|\psi^+\psi^+\psi^+\psi^+\psi^+\rangle$ with a λ_G of 1.40—is likely a result of error disrupting the preparation of the initial state.

N	State	Simulation	Melbourne
4	$\|\phi^+\phi^+\rangle$	1.02	0.94
4	$\|\psi^+\psi^+\rangle$	1.02	0.94
4	$\|\phi^+\psi^+\rangle$	1.02	0.95
6	$\|\phi^+\phi^+\phi^+\rangle$	1.03	0.93
6	$\|\psi^+\psi^+\psi^+\rangle$	1.02	0.95
6	$\|\phi^+\psi^+\phi^+\rangle$	1.02	0.96
8	$\|\phi^+\phi^+\phi^+\phi^+\rangle$	1.03	0.98
8	$\|\psi^+\psi^+\psi^+\psi^+\rangle$	1.03	0.97
8	$\|\phi^+\psi^+\phi^+\psi^+\rangle$	1.03	0.98
10	$\|\phi^+\phi^+\phi^+\phi^+\phi^+\rangle$	1.04	1.09
10	$\|\psi^+\psi^+\psi^+\psi^+\psi^+\rangle$	1.04	1.40
10	$\|\phi^+\psi^+\phi^+\psi^+\phi^+\rangle$	1.03	1.05

TABLE X: Simulated and non-mitigated, experimental λ_G values for N-qubit systems composed of $\frac{N}{2}$ independent $|\phi^+\rangle$ and $|\psi^+\rangle$ Bell states where $N = 4, 6, 8$, and 10 qubits. Experiments were conducted on IBM's Quantum Experience Melbourne (ibmq_16_melbourne) device.

D. $\frac{N}{6}$ Independent Six-Qubit GHZ States in Overall N-Qubit Systems

A six qubit GHZ state on qubits i, j, k, l, p, and q can be prepared using the following gate sequence:

$$C_p^q C_l^p C_k^l C_j^k C_i^j H_i. \tag{7}$$

As such, any N-qubit system such that N is a multiple of six can be prepared to have $\frac{N}{6}$ independent GHZ states by independently applying Eq. (7) to $\frac{N}{6}$ distinct subsets of qubits. For example, for $N = 18$, three distinct six-qubit GHZ states can be constructed by applying Eq. (7) to qubits $0-5$, $6-11$, and $12-17$ independently. This procedure was conducted for $N = 6, 12, 18$, and 24 and was expected to produce one, two, three, and four islands of exciton condensation, respectively, as those are the numbers of independent entangled systems of qubits are prepared in the overall system of N-qubits. The results for the these composite states for simulation and experimentation on IBM's Quantum Experience Rochester (ibmq_rochester) device for $N = 6, 12, 18, 24$ are shown in Table XI. As can be seen, for the simulated computations, the number of islands of condensation was consistent with intuition. Additionally, for $N = 12$ and $N = 24$ qubit experiments, multiple eigenvalues distinctly above one were observed, indicating that—even with the error inherent on the "noisy" real-world device employed—multiple large eigenvalues of the particle-hole RDM is consistent with systems composed of distinct, entangled subsystems.

N	# Islands Expected	Simulation	Rochester
6	1	3.00	1.69
12	2	2.97, 3.03	1.16, 1.21
18	3	2.50, 3.00, 3.51	1.20
24	4	2.50, 2.97, 3.03, 3.51	1.15, 1.80, 1.97

TABLE XI: Simulated and non-mitigated, experimental eigenvalues of the ${}^2\tilde{G}$ which exceed one for N-qubit systems composed of $\frac{N}{6}$ independent 6-qubit GHZ States where $N = 6, 12, 18$, and 24 qubits. Experiments were conducted on IBM's Quantum Experience Rochester (ibmq_rochester) device.

[1] Lipkin, H. J.; Meshkov, N.; Glick, A. J. Validity of many-body approximation methods for a solvable model: (I.) Exact solutions and perturbation theory. *Nucl. Phys. A* **1965**, *62*, 188–198.

[2] Pérez, R.; Cambiaggio, M. C.; Vary, J. P. t expansion and the Lipkin model. *Phys. Rev. C* **1988**, *37*, 2194–2198.

[3] Mazziotti, D. A. Contracted Schrödinger equation: determining quantum energies and two-particle density matrices without wave functions. *Phys. Rev. A* **1998**, *57*, 4219–4234.

[4] Stein, J. Unitary flow of the bosonized large-NLipkin model. *J. Phys. G Nucl. Part. Phys.* **2000**, *26*, 377–385.

[5] Mazziotti, D. A. Exactness of wave functions from two-body exponential transformations in many-body quantum theory. *Phys. Rev. A* **2004**, *69*, 012507.

[6] Pakin, S.; Coles, P. The Problem with Quantum Computers. *Scientific American* **2019**,

[7] Team, Q. Investigating Quantum Hardware Using Quantum Circuits. 2020; `https://qiskit.org/textbook/ch-quantum-hardware/index-circuits.html`.

[8] Preskill, J. Quantum Computing in the NISQ era and beyond. *Quantum* **2018**, *2*, 79.

[9] pyQuil, Introduction to Quantum Computing¶. `http://docs.rigetti.com/en/stable/intro.html#intro`.

[10] Nachman, B.; Urbanek, M.; de Jong, W. A.; Bauer, C. W. Unfolding Quantum Computer Readout Noise. *arXiv* **2019**,

[11] Zhang, Y.; Deng, H.; Li, Q.; Song, H.; Nie, L. Optimizing Quantum Programs Against Decoherence: Delaying Qubits into Quantum Superposition. *2019 International Symposium on Theoretical Aspects of Software Engineering (TASE)* **2019**,

[12] McClure, D. What does the error rate on the IBMQ website mean. 2019; `https://quantumcomputing.stackexchange.com/questions/9073/what-does-the-error-rate-on-the-ibmq-website-mean`.

[13] Magesan, E.; Gambetta, J. M.; Emerson, J. Characterizing quantum gates via randomized benchmarking. *Physical Review A* **2012**, *85*.

[14] Asfaw, A.; Alexander, T.; Nation, P.; Gambetta, J. Get to the heart of real quantum hardware. 2020; `https://www.ibm.com/blogs/research/2019/12/qiskit-openpulse/`.

[15] Gambetta, J.; Sheldon, S. Cramming More Power Into a Quantum Device. 2019; `https://www.ibm.com/blogs/research/2019/03/power-quantum-device/`.

[16] Cross, A. W.; Bishop, L. S.; Sheldon, S.; Nation, P. D.; Gambetta, J. M. Validating quantum computers using randomized model circuits. *Physical Review A* **2019**, *100*.

[17] Gottesman, D. An introduction to quantum error correction and fault-tolerant quantum computation. *Proceedings of Symposia in Applied Mathematics Quantum Information Science and Its Contributions to Mathematics* **2010**, 13–58.

[18] Devore, J. *Probability and Statistics for Engineering and the Sciences*, 8th ed.; Cengage Learning, 2012; p 267–299.